https://doi.org/10.5194/acp-2020-198
Preprint. Discussion started: 12 March 2020


Atmospheric Chemistry and Physics Discussions

# Effects of atmospheric circulations on the interannual variation in $PM_{2.5}$ concentrations over the Beijing-Tianjin-Hebei region in 2013-2018

Xiaoyan Wang*[1,2], Renhe Zhang[1,2]

1. Department of Atmospheric and Oceanic Sciences & Institute of Atmospheric Sciences, Fudan University, Shanghai, China
2. Big Data Institute for Carbon Emission and Environmental Pollution, Fudan University, Shanghai, China

Correspondence to: wangxyfd@fudan.edu.cn

## Abstract

The Chinese government has made many efforts to mitigate fine particulate matter ($PM_{2.5}$) pollution in recent years by taking strict measures on air pollutants reduction, which has generated the nationwide improvements in air quality since 2013. However, under the stringent air pollution controls, how $PM_{2.5}$ concentration varies and how much the meteorological conditions contribute to the interannual variations in $PM_{2.5}$ concentrations are still unclear, which is very important for the local government to assess the emission reduction of previous year and adjust mitigation strategies of next year. The effects of atmospheric circulation on the interannual variation in wintertime $PM_{2.5}$ concentrations over the Beijing-Tianjin-Hebei (BTH) region in the period of 2013-

https://doi.org/10.5194/acp-2020-198
Preprint. Discussion started: 12 March 2020


Atmospheric Chemistry and Physics Discussions

2018 are evaluated in this study. Generally, the transport of clean and dry air masses and unstable boundary layer working with the effective near-surface horizontal divergence or pumping action at the top of the boundary layer benefit for the horizontal or vertical diffusion of surface air pollutants. Instead, the co-occurrence of a stable boundary layer, frequent air stagnation, positive water vapor advection and deep near-surface horizontal convergence exacerbate the air pollution. Favorable circulation conditions lasting for 2~4 days are beneficial for the diffusion of air pollutants, and 3~7 days of unfavorable circulation events exacerbate the accumulation of air pollutants. The occurrence frequency of favorable circulation events is consistent with the interannual variation in seasonal mean $PM_{2.5}$ concentrations. There is better diffusion ability in the winters of 2014 and 2017 than in other years. A 76.5% of the observed decrease in $PM_{2.5}$ concentrations in 2017 over the BTH region could be attributed to the improvement in atmospheric diffusion conditions. It is essential to exclude the contribution of meteorological conditions to the variation in interannual air pollutants when making a quantitative evaluation of emission reduction measurements.

## Introduction

Rapid economic development and associated emissions have led to recent severe air pollution over China, which has become a central issue of concern for the public and governments (Wang et al., 2018; Zhang et al., 2014; Song et al., 2018; Mu and Zhang, 2014; Tao et al., 2018). High levels of fine particulate matter ($PM_{2.5}$) concentrations influence people's daily lives and threaten public health (Liu et al., 2019; Zhao et al., 2018a; Hong et al., 2019; Zhang et al., 2017). In addition, they are efficient in scattering and absorbing solar radiation, and are involved in the climate change by changing the surface energy budget (Wang et al., 2009; Wang et al., 2017; Bi et al., 2016; Chen et al., 2019b; Li et al., 2018; Zhao et al., 2019b; Che et al., 2019). To mitigate $PM_{2.5}$ pollutions, the Chinese government issued the Air Pollution Prevention and Control Action Plan (hereinafter referred to as the Clean Air Action hereinafter) in 2013, which required the Beijing-Tianjin-Hebei (BTH) region, Yangtze River Delta and Pearl River Delta to reduce their $PM_{2.5}$ concentrations by 15~25% from 2013 to 2017 (China's State Council, 2013). A series of stringent clean air actions was implemented to improve air quality, including strengthening industrial emission standards, phasing out small and

https://doi.org/10.5194/acp-2020-198
Preprint. Discussion started: 12 March 2020


Atmospheric Chemistry and Physics Discussions

polluting factories, strengthening vehicle emission standards and more (Zhang and Geng, 2019). To further improve air quality, the state council has released a three-year action to win the battle for a blue sky in 2018, solidifying a timetable and roadmap for improving air quality. By 2020, emissions of sulfur dioxide and nitrogen oxides are required to decline by at least 15% from 2015 levels, while cities with low air quality standards should see their $PM_{2.5}$ density fall by at least 18%, according to the plan (China's State Council, 2018). To achieve these goals, many efforts have focused on adjustments to industrial, energy and transportation structures involved with central to local government.

With the implementation of the toughest-ever clean air actions from Clean Air Action, the anthropogenic emissions show significant decreased by 59% for $SO_2$, 21% for NOx, 23% for CO, 36% for $PM_{10}$ and 33% for primary $PM_{2.5}$ from 2013 to 2017 (Zheng et al., 2018; Wang et al., 2019b). As a consequence, air quality in China improved significantly in terms of annual mean $PM_{2.5}$ concentrations, polluted days and pollution durations from 2013 to 2017, and surpassed the mitigation targets of the Clean Air Action (Fan et al., 2020; Zhao et al., 2018b; Gui et al., 2019; Zhong et al., 2018). By the end of 2017, the BTH region achieved its primary goal of reducing the annual average $PM_{2.5}$ concentration to less than 60 $\mu g/m^3$ with a decreasing trend of -9.3±1.8 $\mu g/m^3$ (Wang et al., 2019b). However, in addition to air pollutants emissions, atmospheric meteorological conditions play an important role in the transport, accumulation, scavenging and chemical production of particles, which drives the evolution of every air pollution episode (Zhang et al., 2012; Leung et al., 2018; Huang et al., 2018; Wang et al., 2016). Moreover, the interannual to interdecadal variations in meteorological or climate signals (e.g., monsoon intensity, variation in sea ice, and the occurrence of El Niño Southern Oscillation (ENSO) and North Atlantic Oscillation (NAO)) also have significant effects on the variation in ambient $PM_{2.5}$ concentrations (Li et al., 2016; Chen et al., 2019a; Zhao et al., 2018c; Dang and Liao, 2019; Feng et al., 2019; Yin et al., 2019). The global warming associated with climate change may also contribute to the air pollution in China (Cai et al., 2017; Zhang, 2017).

Recently, many researchers investigated how much of the recent decreased $PM_{2.5}$ concentrations could be attributed to the contribution to emission reduction compared to the effects of atmospheric

https://doi.org/10.5194/acp-2020-198
Preprint. Discussion started: 12 March 2020


Atmospheric Chemistry and Physics Discussions

elements. The studies have been carried out to evaluate the relative effects of emission reduction and meteorological conditions on the recent decrease in $PM_{2.5}$ concentrations (Ding et al., 2019; Guo et al., 2019; He et al., 2018; Zhang et al., 2019c; Zhao et al., 2019a). Based on a multiple linear regression model, 12% of the decreased $PM_{2.5}$ over China is due to favorable meteorological conditions between 2013 and 2018 (Zhai et al., 2019). For the BTH region, Zhang et al. (2019b) used the parameter linking air quality and meteorology (PLAM) index (a meteorological pollution index for air quality) to evaluate meteorological conditions, and found that only approximately 5% of the 39.6% reduction in $PM_{2.5}$ in 2017 could be attributed to meteorological changes. The relative contribution of emission reduction to the decreased $PM_{2.5}$ concentrations in Beijing calculated by the statistical model and Weather Research and Forecasting-Community Multiscale Air Quality (WRF-CMAQ) was 80%, indicating that emission reductions were crucial for air quality improvement in Beijing from 2013 to 2017 (Chen et al., 2019c). In addition, Zhang et al. (2019a) quantified the contribution of different emission control policies to the rapid improvement in $PM_{2.5}$ pollution over China from 2013 to 2017 and highlighted the significant effects of strengthening industrial emission standards and upgrading industrial boilers on air quality improvement during the Clean Air Action.

Based on the investigation of different methods, the effectiveness of emission mitigation actions was confirmed to drive the recent remarkable improvement in air quality in China since 2013. However, most of the existing studies have focused on the relative long-term variation of air quality (i.e., five to six years since 2013) and evaluated emission reduction effects over a multiyear time scale. The Chinese government took a series of steps to reduce air pollutant emissions, which requires a certain sacrifice regarding economic growth. In this situation, the local government need an accurate evaluation of the emission reduction effects during the previous year and reasonable adjustment of the mitigation policies of next year to keep the balance of economic growth and environmental protection. The accurate evaluation of emission reduction effects should exclude the meteorological element contribution to the interannual variations of air quality. Therefore, the contribution of meteorological conditions to the interannual variation in wintertime $PM_{2.5}$ concentrations over the BTH region will be discussed in this study.

https://doi.org/10.5194/acp-2020-198
Preprint. Discussion started: 12 March 2020


Atmospheric Chemistry and Physics Discussions

## 2. Data and Methods

### 2.1 On-site $PM_{2.5}$ mass concentration

The wintertime (December to February of the following year) hourly observed $PM_{2.5}$ mass concentration dataset over China from 2013 to 2018 was provided by the Ministry of Ecology and Environment of the People's Republic of China (http://106.37.208.233:20035). This study mainly focuses on the region of BTH region (113.5º-119ºE and 36º-42.5ºN, the solid-line box in Fig. 3), and 114 $PM_{2.5}$ stations are available over this region. The hourly $PM_{2.5}$ concentration was averaged to the daily mean value with no more than 40% missing data.

### 2.2 Method of atmospheric circulation classification

Commonly used objective classification methods include correlation, clustering, nonlinear methods, principal component analysis (PCA), and fuzzy analysis. Huth et al. (2008) compared these five classification methods and proposed that the performance of the T-mode PCA was the best in terms of its reproduction of predefined types, temporal and spatial stabilities, and reduced dependence on preset parameters. The T-mode PCA has been successfully applied to studies of general circulation models (Huth, 2000), climate change (Cavazos, 2000), and local air pollution (Xu et al., 2016; Valverde et al., 2015; Miao et al., 2017; Li et al., 2019). Zhang et al. (Zhang et al., 2012) first employed the obliquely rotated T-mode PCA method developed by COST action 733 (http://www.cost733.org) (Philipp et al., 2014) to identify the circulation pattern that is conductive to PM pollution in North China. In this study, the four-times-daily dataset of the fifth generation European Centre for Medium-Range Weather Forecasts (ECMWF ERA5) atmospheric reanalysis in winters from 2013 to 2018 with a horizontal resolution of 0.25º was used for synoptic circulation classification. The daily mean geopotential height fields at 925, 850 and 500 hPa were applied to the T-mode PCA method in the Cost733 toolbox. Our target region is 105º-125ºE and 30º-55ºN (the dashed box in Fig. 3).

https://doi.org/10.5194/acp-2020-198
Preprint. Discussion started: 12 March 2020


Atmospheric Chemistry and Physics Discussions

134 **2.3 Model simulation**

135 The regional chemical/transport model WRF chemical model (WRF-Chem) version 4.0, was
136 applied to simulate the effects of meteorological condition variation on seasonal air pollution over
137 northern China at a horizontal resolution of 9 km (245*220 horizontal grid cells) and vertical
138 resolution of 33 layers. The simulation domain covers most areas of the North China region (Fig.
139 10). The initial and lateral meteorological boundary conditions are derived from the NCEP FNL
140 reanalysis data every 6 hours. The chemical and aerosol mechanisms used were the RADM2
141 chemical mechanism from Stockwell et al. (1990) and MADE/SORGAM aerosols (Ackermann et
142 al., 1998; Schell et al., 2001). MADE/SORGAM are used to simulate all major aerosol components
143 including sulfate, nitrate, ammonium, black carbon, organic carbon, sodium, chloride, mineral dust,
144 and water content. Madronich photolysis was used to calculate photochemical reactions. Other
145 major physical processes included the CAM shortwave radiation (Collins et al., 2004), RRTMG
146 longwave radiation (Iacono et al., 2008), the unified Noah land-surface model land surface option
147 and MYJ planetary boundary layer parameterization (Janjić, 1994).

148 To evaluate the impacts of meteorological contributions on the $PM_{2.5}$ variation between the 2016
149 winter (Dec. 2016 to Feb. 2017) and 2017 winter (Dec. 2017 to Feb. 2018) over the BTH region,
150 we conducted two sensitivity runs: the same emissions as the 2016 winter and the actual
151 meteorological conditions of 2016 and 2017. Thus, the difference in the simulated $PM_{2.5}$
152 concentrations between the 2016 and 2017 winters could be attributed to the meteorological
153 variation. The anthropogenic emission inventory for 2016 developed by Tsinghua University was
154 used in this study (available at http//www.meicmodel.org), as is named the Multiresolution
155 Emission Inventory for China (MEIC), containing monthly anthropogenic emissions of $SO_2$, NOx,
156 CO, $NH_3$, $PM_{2.5}$, PMcoarse, BC, OC and NMVOCs. The horizontal resolution of the MEIC used
157 in this study is 0.25°. Each simulation is initialized at 00:00 UTC on Nov. 15, and the first 15-day
158 simulations are regarded as the spin-up period. Daily mean $PM_{2.5}$ concentrations between Dec. 1,
159 2016 to Feb. 28, 2017, and Dec. 1, 2017 to Feb. 28, 2018, are used to investigate the effects of
160 meteorological conditions on seasonal air pollution.

161

https://doi.org/10.5194/acp-2020-198
Preprint. Discussion started: 12 March 2020


Atmospheric Chemistry and Physics Discussions

## 3. Results

### 3.1 Dominate synoptic circulation types in winter over the BTH region

As shown in Fig.1, the wintertime $PM_{2.5}$ concentrations over the BTH region show a remarkable decrease from 2013 to 2018 due to a series of air pollution reduction measures. Compared to 2013, the mean $PM_{2.5}$ concentration for 2018 decreased by 35.6% over 114 stations around the BTH region (cf. Table 1). However, under the background of improved air quality, evident interannual variations in $PM_{2.5}$ concentrations have been observed in recent years. The $PM_{2.5}$ concentrations in the winters of 2016 and 2018 are higher than those in the same period of the previous year, with mean values increasing by 18% and 13.36%, respectively. The high emissions of primary fine particulate matters and its precursors are considered as internal factors of severe $PM_{2.5}$ pollution in China; thus, emission reduction is the most direct and effective way to improve local air quality. However, the evolution of each air pollution episode is strongly affected by the local synoptic circulation pattern. Both emissions and atmospheric conditions are related to the ambient $PM_{2.5}$ concentration level. It is essential to exclude the atmospheric circulation impacts on air quality when assessing emission mitigation effects.

We use synoptic circulation types to measure the ability of atmospheric circulation to the accumulate, remove, and transport air pollutants. The daily mean geopotential height fields at 925, 800 and 500 hPa in the winters of 2013 to 2018 (total of 451 days) are used to conduct objective synoptic circulation classification based on the T-mode PCA method with the Cost733 toolbox. Three levels of geopotential height fields (i.e., 925 850 and 500 hPa) in the lower to middle troposphere over 105º-125ºE and 30º-55ºN are used in circulation type (CT) classification. Six typical synoptic circulation types (CTs) are identified during winter in the BTH region, with a total explained variance of 70% (Fig. S1). The horizontal (i.e., sea level pressure (SLP), wind, relative humidity (RH) and boundary layer height (BLH)) and vertical (i.e., atmospheric stability, vertical velocity, temperature and divergence) distributions of meteorological variables are used to illustrate the mechanism behind CT effects on air pollution. To obtain a broad view of the six CTs, the horizontal distribution of atmospheric circulation patterns, as shown in Fig. 2 and Fig. 3 cover a larger area

https://doi.org/10.5194/acp-2020-198
Preprint. Discussion started: 12 March 2020


Atmospheric Chemistry and Physics Discussions

than the area used in the CT classification with the Cost733 toolbox.

Fig. 2 and Fig. 3 exhibit the original and anomalous patterns of the mean SLP and surface wind field of each CT, respectively. CT1 is the most frequent CT during the study period with an occurrence frequency of 33% based on the results of the Cost733 classification. CT1 shows that a high-pressure system originates in the Siberian region extending along central Inner Mongolia to southern China. Northwesterly winds prevail in northern China and turn into northerly winds in southern China. The mean wind speed is 3.27 m/s over the BTH region (cf. Table 2), which is the highest among the six CTs and benefits the outward transport of local air pollutants. Fig. 3 shows the SLP and surface wind anomalies of each CT. In the CT1 situation, the BTH region is located west of the cyclonic anomaly, which is dominated by an obvious northwesterly wind anomaly. The wind field pattern corresponds to the negative RH anomaly over the BTH region in Fig. 4. The vertical profiles of dynamic and thermodynamic stratification are included to investigate vertical diffusion. Based on the vertical distribution of atmospheric stability shown in Fig. 5, atmospheric stratification is characterized by a stable layer at the top of the boundary layer for all the cases. For CT1, an obvious unstable stratification occurs at the bottom of boundary layer over the BTH region, which enhances the turbulent activities and is beneficial for the vertical diffusion of air pollutants. The unstable boundary layer is also confirmed by the positive BLH anomaly and elevated negative temperature anomaly, as shown in Fig. S2 and Fig. S3. Fig. S4 shows a strong surface divergence and strong top convergence vertical pattern in CT1, which generates sinking movement over the BTH region. As shown in Fig. 6, a subsidence anomaly appears at the lower to middle troposphere over the BTH region with a mean descending velocity of 0.04 pa/s between 850 and 1000 hPa. The strong downdraft brings a clean and dry air mass to the surface and increases the horizontal divergence of surface air pollutants (shown in Fig. S4). The cold, clean and dry air mass transported by the surface northwesterly winds, unstable boundary layer and strong horizontal divergence are favorable for the improvement in ambient air quality.

The occurrence frequency of CT2 is 11%. As shown in Fig. 2, a high-pressure system around Baikal is obvious under the CT2 condition, which is stronger and further east than CT1. The BTH region is located at the ridge of the high-pressure system with weak northwesterly winds occurring in the

https://doi.org/10.5194/acp-2020-198
Preprint. Discussion started: 12 March 2020


Atmospheric Chemistry and Physics Discussions

northern BTH region, which turn to northeasterly in the southern BTH region. The anomalous fields in Fig. 3 show a large area of a positive SLP anomaly over the north of 40ºN. The BTH region is just located at the south edge of the anticyclone anomaly with prevailing northeasterly surface wind. Fig. 4 shows a weak negative RH anomaly over the BTH region due to the dry wind from the northeast. Similar to CT1, CT2 also shows an unstable stratification in the boundary layer, which increases the vertical diffusion of air pollution. Both the weak positive BLH anomaly and elevated negative temperature anomaly indicate the enhanced instability of the atmospheric boundary layer (Figs. S2-S3). Intense updraft is stimulated by strong convergence at the surface working with strong divergence at the top of the boundary layer, as shown in Fig. S4. As shown in Fig. 6, upward movement dominates in the middle-low troposphere over the BTH region with a mean ascending velocity of 0.0358 pa/s between 850 and 1000 hPa. Although the elevated temperature stability is relatively strong in CT2, the bottom-up updraft breaks through the stable layer and brings the surface air pollutants to the free atmosphere. In summary, the unstable boundary layer working with the upper divergence pumping action enhances the vertical diffusion of surface air pollutants, which will decrease the surface concentrations of air pollutant.

CT3 shows a relatively uniform SLP distribution with a weak pressure gradient over the BTH region as shown in Fig. 2. The prevailing westerly wind hinders the southward transport of the cold air mass to some extent. The cyclonic anomaly with southwesterly wind can be found over the BTH region. As shown in Fig. 3, the southwesterly wind transports the upstream air pollutants and warm moisture to the BTH, which accelerates the hygroscopic growth of particles, promotes the gas-to-particle transformation and increases the local air pollutant concentration (Wang et al., 2019a). The positive RH and temperature anomaly in Fig. 4 and Fig. S3 correspond to the southwesterly wind anomaly. Unlike to CT1 and CT2, CT3 shows a stable stratification below 700 hPa. In addition, the upper unstable stratification of CT3 is lower than that of CT1 and CT2, indicating a negative BLH anomaly (as shown in Fig. S2). CT3 also shows upward movement over the BTH region, but it is weaker than CT2 by one order of magnitude. By contrast, the effects of the stronger near-surface convergence will offset the upward transport, which will increase the local air pollutants. The stable boundary layer, southeasterly warm moisture and effective convergence aggravate local air pollution.

https://doi.org/10.5194/acp-2020-198
Preprint. Discussion started: 12 March 2020


Atmospheric Chemistry and Physics Discussions

For the cases of CT4 and CT5, the BTH region is co-located with a weak surface anticyclone with low average surface winds of 2.24 and 2.58 m/s, respectively. The calm surface winds coexisting with the lower BLHs (cf. Fig. S2) decrease the ventilation coefficient and increase the occurrence of air stagnation conditions. The surface anomaly fields show southeasterly and southerly winds in CT4 and CT5, respectively. As shown in Fig. 4, the northward wind anomaly increases the humidity and air pollutants of the BTH region. Based on the vertical profiles of temperature and atmospheric stability, an elevated positive temperature anomaly increases the stability of the boundary layer, thus reducing the vertical diffusion of air pollutants. The weak near surface convergence could increase the accumulation of air pollution, but moderate upward movement will bring the surface air pollutants to the outside of the boundary layer, which offsets the surface convergence to some extent. CT4 and CT5 had the same occurrence of 15% during the study period. Although the CT4 and CT5 show different large-scale surface circulation patterns, the meteorological variables over the BTH region are almost the same. The air stagnation conditions and southerly water vapor transport result in the accumulation and hygroscopic growth of particles.

In terms of CT6, the BTH region is located at the ridge of the Mongolian anticyclone, and its high-pressure system is weaker than that of CT2. The prevailing wind turns from northwest to northeast over the BTH region. As shown by the surface meteorological anomaly distribution, the BTH region is situated at the border between the northern anticyclonic and southern cyclonic anomalies with prevailing northeasterly wind coming from the Bohai Sea. A large amount of water vapor from the sea plays an important role in the hygroscopic growth of particles over the BTH region. Fig. 5 indicates a stable boundary layer when CT6 occurs, which reduces the vertical diffusion of surface air pollutants. CT6 shows a deep horizontal convergence under 850 hPa, which is favorable for the accumulation of moisture and air pollutants. The effect of the relatively weak divergence above strong convergence is not distinct for the improvement in surface air quality. Therefore, the circulation pattern of warm moist flow from the sea, a stable boundary and effective horizontal convergence exacerbates local air pollution.

### 3.2 Atmospheric circulation pattern effects on air quality

The potential mechanisms of the CT effects on local air quality are discussed in the last section.

https://doi.org/10.5194/acp-2020-198
Preprint. Discussion started: 12 March 2020


Atmospheric Chemistry and Physics Discussions

Combinations of the following situations are favorable for the improvement in air quality: transport of a clean and dry air mass, unstable boundary layer, effective horizontal divergence and vertical transport of air pollutants to the free atmosphere. In contrast, the positive humidity anomaly, stable boundary layer, frequent air stagnation conditions and deep horizontal convergence exacerbate air pollution.

To exclude the effects of interannual variation in air quality due to the emission reduction background, the daily $PM_{2.5}$ concentration distribution displayed by year and CT, as shown in Fig. 7 reveals the effects of CT on air quality. The mean and median values of $PM_{2.5}$ concentrations during each CT are summarized in Table 1. The mean and median $PM_{2.5}$ concentrations in the CT1 condition are both lower than the seasonal mean and median for all years. Under the CT2 condition, the $PM_{2.5}$ concentrations are also lower than the seasonal mean except for 2014. However, the $PM_{2.5}$ concentrations are generally higher than the seasonal mean in CT3-CT6. As for the multiyear average, it shows distinctly lower $PM_{2.5}$ concentrations in CT1 and CT2 than the other CTs. Based on the $PM_{2.5}$ concentration in each CT, CT1 and CT2 can be considered as favorable CTs for air quality, which are beneficial for the diffusion of air pollutants, and CT3-CT6 are unfavorable CTs, which exacerbate air pollution.

Giving the above analysis, $PM_{2.5}$ concentration tended to be lower than normal when a favorable CT occurred, and vice versa. Therefore, the occurrence frequency of each CT plays an important role in air quality during the study period. CT1 and CT2 are combined as the favorable circulation, and CT3-CT6 are referred to as the unfavorable circulation. Fig. S5 exhibits the seasonal occurrences of favorable and unfavorable circulation types. Fifty-four days of unfavorable circulation occurred in winter 2013, which is the greatest frequency during the study period. A higher unfavorable circulation frequency was also shown in 2014 and 2018 winters. In contrast, the favorable circulations were much higher in 2015 and 2017 winters than in the other winters. The seasonal frequencies of favorable and unfavorable circulations are in line with the trend in seasonal $PM_{2.5}$ concentrations. It is worth noting that although the seasonal mean $PM_{2.5}$ concentration in the winter of 2015 (Dec. 2015 to Feb. 2016) is lower than that of 2014, but the $PM_{2.5}$ concentration in Dec. 2015 is much higher than that in Dec. 2014. The high $PM_{2.5}$ concentration in Dec. 2015 is

https://doi.org/10.5194/acp-2020-198
Preprint. Discussion started: 12 March 2020


Atmospheric Chemistry and Physics Discussions

consistent with the high frequency of unfavorable CTs during that time, which indicates the robustness of circulation classification.

However, every air pollution event has a duration from the development to decay stage. Generally, several days are needed for the accumulation of air pollutants, followed by a relatively quick removal. The variation in meteorological conditions controls the evolution of each air pollution episode. Therefore, the duration of each CT determines the duration of the air pollution event. Fig. 8 exhibits the variation in the $PM_{2.5}$ concentration anomaly with the duration of favorable and unfavorable CTs. As discussed above, the favorable circulations generally correspond to the negative $PM_{2.5}$ concentration anomaly (lower than the monthly mean), while the unfavorable circulations result in a positive $PM_{2.5}$ concentration anomaly. When the favorable circulation duration shorter than 4 days, the absolute values of the negative anomaly of $PM_{2.5}$ concentrations increase with the duration of favorable circulation; however, with the continuous increase in favorable circulation durations, the magnitude of the negative anomaly of $PM_{2.5}$ concentrations slightly decreases and remains unchanged. Similarly, the positive anomalies of the $PM_{2.5}$ concentrations increase with the duration of unfavorable circulation durations when the duration is less than 7 days. However, the effect of circulation on air pollutant diffusion is not obvious when a one-day favorable or one-two-day unfavorable circulation occurs. That is favorable CTs lasting 2~4 days are beneficial for the diffusion of air pollutants; and unfavorable circulation events lasting 3~7 days exacerbate the accumulation of air pollutants.

The occurrences of 2~4 days favorable circulation and 3~7 days of unfavorable CTs are shown in Fig. 9. It shows a high frequency of 2~4 days of favorable circulation in 2017 and 2014 with totally 15 and 13 days, respectively. The favorable circulation occurrences are lower in the winters of 2016 and 2018 than in the other winters. In terms of the 3~7 days of unfavorable circulations, the years of 2013, 2016 and 2018 show higher frequencies than the other years. Therefore, based on the occurrence of favorable and unfavorable CTs, the atmospheric diffusion abilities are better in 2014 and 2017 than in the other years. The significant improvement in air quality in 2014 and 2017 is consistent with the improvement in atmospheric diffusion abilities compared to their previous years.

https://doi.org/10.5194/acp-2020-198
Preprint. Discussion started: 12 March 2020


Atmospheric Chemistry and Physics Discussions

### 3.3 Contributions of atmospheric diffusion condition variations to the $PM_{2.5}$ concentration decrease between 2016 and 2017

Although the interannual variation in $PM_{2.5}$ concentrations show good correlation with the occurrence of favorable or unfavorable circulation, Sec. 3.2 is just a qualitative analysis. Taking the interannual variation in $PM_{2.5}$ concentrations between 2016 and 2017 as an example, the model simulation based on the WRF-Chem model is used to evaluate the quantitative contributions of meteorological condition variations to the $PM_{2.5}$ concentration decrease in 2017. The emissions are fixed in 2016 (Dec. 2016 to Feb. 2017), and the meteorological fields come from the NECP GDAS Final Analysis dataset for the 2016 and 2017 winters, respectively. The meteorological fields and air pollutants over some cities from north to south in the simulated domain (i.e., Shijiazhuang, Beijing, Tianjin, Xuzhou and Shanghai) are included to evaluate the performance of the model simulation. Fig. S6 shows the variations in the observed and simulated daily mean air temperature, sea level pressure, relative humidity and surface wind speed from Jan. to Feb. of 2017. Although the model slightly overestimates the surface wind speed over Shijiazhuang and Shanghai, most of the simulated meteorological variables agree well with the observations over all cities. For the concentration of air pollutants in Fig. S7, the model generally underestimates the $PM_{2.5}$ concentrations under highly polluted conditions, with a bias of 44.9%~59.6% (different cities) when the observed $PM_{2.5}$ was higher than 75 $\mu g/m^3$. However, the bias between the simulated and observed $PM_{2.5}$ concentrations decreased to 12.4%~26.8% at lower $PM_{2.5}$ concentration level. Due to the deficiency of the PBL scheme (Tie et al., 2015), the heterogeneous/aqueous process in the model (Li et al., 2011) and uncertainty in the emission inventory, current air quality models show limited capacity in severe air pollution episodes. However, the day-to-day variation in all the air pollutants can be well captured by the WRF-Chem model, with the highest correlation coefficient of 0.76 between the observed and simulated $PM_{2.5}$ in Xuzhou. Overall, both the meteorological variables and air pollutants are well reproduced by the WRF-Chem model, which provides confidence for further discussions.

The simulated seasonal mean $PM_{2.5}$ concentrations of the 2016 and 2017 winters are presented in Fig. S8. It shows a significant spatial distribution of seasonal $PM_{2.5}$ concentrations with higher

https://doi.org/10.5194/acp-2020-198
Preprint. Discussion started: 12 March 2020


Atmospheric Chemistry and Physics Discussions

concentrations over the BTH region, Shandong and Henan Provinces. Even though the emissions were set to the level of 2016, the simulated seasonal $PM_{2.5}$ concentrations in 2016 were much higher than those in 2017 due to the difference in meteorological fields. Fig. 10 exhibits the observed and simulated $PM_{2.5}$ concentration differences between 2017 and 2016. Both the observations and simulations show significant negative growth in $PM_{2.5}$ concentrations over northern China from 2016 to 2017 in winter but relatively weak positive growth over the lower Yangtze River Delta. The BTH region is located at the center of negative growth, with an observed average of 46.3 $\mu g/m^3$ decrease of $PM_{2.5}$ concentration from 2016 to 2017. While, the simulated difference of $PM_{2.5}$ between 2016 and 2017 winter is -8.4 $\mu g/m^3$, which is much lower than the observed value. The absolute $PM_{2.5}$ concentration would be underestimated because of the limited performance of the WRF-Chem model under severe air pollution; therefore, the relative differences between 2016 and 2017 are involved to evaluate the effects of meteorological field variations on the decrease in $PM_{2.5}$ concentrations. Based on the relative difference in $PM_{2.5}$ concentration between 2016 and 2017, the observed difference at 114 stations over the BTH region is -37.1% compared to the mean value of 2016 winter, and the averaged simulated difference is -28.4% over the region of 113º-117.5ºE and 36º-42ºN, which is due to the difference in meteorological conditions. Thus, 76.5% of the observed 37.1% decrease in $PM_{2.5}$ concentration in 2017 over the BTH region could be attributed to the improvement in atmospheric diffusion conditions. The variation of meteorological conditions plays an important role in the interannual variation in air pollutant concentrations.

## 4. Conclusions and Discussion

Recent severe $PM_{2.5}$ pollution in China has aroused unprecedented public concern. The Chinese government has implemented many emission reduction measurements, which has greatly improved the air quality recently. The wintertime $PM_{2.5}$ concentration of 2018 decreased by 35.6% compared to 2013 over the BTH region. However, there was obvious interannual variation in $PM_{2.5}$ concentrations from 2013 to 2018. Atmospheric circulation classification method based on the Cost733 toolbox is used to investigate the mechanism behind atmospheric circulation effects on air pollutant diffusion. Six CTs are identified during the winters from 2013 to 2018 over northern China,

https://doi.org/10.5194/acp-2020-198
Preprint. Discussion started: 12 March 2020


Atmospheric Chemistry and Physics Discussions

and two of which are considered as favorable circulations for air pollutant diffusion and the other four CTs exacerbate local air pollution. Generally, the transport of clean and dry air mass and unstable boundary layers working with the effective near-surface horizontal divergence or pumping action at the top of the boundary layer will benefit for the horizontal or vertical diffusion of surface air pollutants. However, the co-occurrence of a stable boundary layer, frequent air stagnation, positive water vapor advection and deep near-surface horizontal convergence exacerbates the air pollution.

Except for the atmospheric circulation characteristic of CTs, the durations of each circulation type also have a great influence on the local air quality. The one-day favorable or less than two-day unfavorable circulations have no significant effects on the diffusion and accumulation of air pollutants. Comparatively speaking, favorable CTs lasting for 2~4 days are beneficial for the diffusion of air pollutants, and the 3~7 days of unfavorable circulation events exacerbate the accumulation of air pollutants. The occurrences of 2~4 days of favorable and 3~7 days of unfavorable circulation are used to evaluate the atmospheric diffusion ability, which shows better diffusion abilities in 2014 and 2017 than in the other years. Taking the decrease of $PM_{2.5}$ concentration between 2016 and 2017 as an example, 76.5% of the decreased concentration over the BTH region could be attributed to the improvement in atmospheric diffusion conditions of 2017. The variation in meteorological conditions plays an important role in the interannual variation in air pollutant concentrations. The 2020 is the key and target year for the three-year action to win the battle for a blue sky of 2018. It is essential to exclude the contribution of meteorological conditions to the variation in interannual air pollutants when making a quantitative evaluation of emission reduction measurements.

**Acknowledgments:** This study was supported by the National Natural Science Foundation of China (41790470 and 41805117).

**Code/Data availability:** The release version 4.0 of WRF-Chem can be download from http://www2.mmm.ucar.edu/wrf/users/download/get_source.html. Hourly $PM_{2.5}$ concentration

https://doi.org/10.5194/acp-2020-198
Preprint. Discussion started: 12 March 2020


Atmospheric Chemistry and Physics Discussions

observations were obtained from the website of Ministry of Ecology and Environment of the People's Republic of China (http://106.37.208.233:20035). Daily four times ECMWF ERA5 dataset during 2013 to 2018 are downloaded from https://www.ecmwf.int/en/forecasts/datasets/reanalysis-datasets/era5. Hourly observations of meteorological variables used for the WRF-Chem simulation evaluations are downloaded from the Intergrated Surface Database of National Climate Data Center (https://www.ncdc.noaa.gov/isd).

**Competing interests:** The authors declare that they have no conflict of interest.

**Author contributions:** Wang X. and Zhang R. designed research; Wang X. performed the analyses and wrote the paper; All authors contributed to the final version of the paper.

https://doi.org/10.5194/acp-2020-198
Preprint. Discussion started: 12 March 2020


Atmospheric Chemistry and Physics Discussions

## Figure Captions:

Figure 1. Interannual variation in the wintertime $PM_{2.5}$ concentrations at 114 stations over the BTH region. In each box, the central mark indicates the median, and the bottom and top edges of the box indicate the 25th and 75th percentiles, respectively. The whiskers extending to the most extreme data points are considered outliers. The region covered by the blue box in Fig. 2 is considered as the BTH region (113º-117.5ºE and 36º-42ºN).

Figure 2. The distribution of sea level pressure (shaded, unit: pa) and 10 m wind fields (vector, unit: m/s) in each circulation type. The number over each subplot indicates the occurrence frequency of the specific circulation type. The solid blue box is the location of BTH region. The daily mean geopotential height fields at 925, 850 and 500 hPa over the dashed blue box (105º-125ºE and 30º-55ºN) were applied to T-mode PCA method with the cost733 toolbox. The region mean wind speed of each circulation type is shown in Table 2.

Figure 3. The distribution of sea level pressure (unit: pa) and 10 m wind fields (unit: m/s) anomaly in each circulation type. The anomaly values are with respect to the 1980-2010 mean. Regional mean wind speed anomaly of each circulation type is summarized in Table 2.

Figure 4. The distribution of relative humidity in each circulation type (unit: %). The anomaly values are with respect to the 1980-2010 mean.

Figure 5. Zonal profile of temperature lapse rate over the BTH region (36º-42ºN) (unit: K/100 m). The gray region indicates the average altitude over 36º-42ºN. The region between the two dashed lines is the horizontal location of the BTH region (113º-117.5ºE).

Figure 6. Zonal vertical profile of vertical velocity anomaly over BTH region (unit: pa/s). The anomaly of the vertical velocities is with respect to the 1980 to 2010 mean value.

Figure 7. The box plot of the $PM_{2.5}$ concentrations varies with the circulation types. To exclude the effect of emission reduction on the annual mean $PM_{2.5}$ concentrations, the $PM_{2.5}$ distributions at the year and multiyear (average) scales are shown here, respectively. The dashed line for each year indicates the median $PM_{2.5}$ concentrations in wintertime of a specific year.

Figure 8. The daily $PM_{2.5}$ concentration anomalies vary with favorable (F) and unfavorable (U) event durations. The occurrences of CT1 and CT2 are collectively called favorable events, and CT3 to CT6 are referred to as unfavorable events. U1 indicates an unfavorable circulation event lasting for one day, and U2 means a two-day event. The central red line in each box indicates the median, and the circle is the mean value.

Figure 9. Occurrence frequencies of the effective favorable and unfavorable events. The effective favorable events referred to the favorable events lasting for two to four days. The effective unfavorable events indicate the unfavorable

https://doi.org/10.5194/acp-2020-198
Preprint. Discussion started: 12 March 2020


Atmospheric Chemistry and Physics Discussions

events lasting for three to seven days. The specific number of days for favorable/unfavorable events is shown on the top of each bar.

Figure 10. Distributions of the observed and simulated $PM_{2.5}$ difference between the winters of 2016 and 2017. The left panel is the absolute value (unit: $\mu g/m^3$) and the right panel is the relative difference with respect to the mean value of 2016 (unit: %). The simulated seasonal mean $PM_{2.5}$ concentrations during the two years are shown in Fig. S8.

https://doi.org/10.5194/acp-2020-198
Preprint. Discussion started: 12 March 2020


Atmospheric Chemistry and Physics Discussions

462 Table 1. The seasonal mean and median $PM_{2.5}$ concentrations in each atmospheric circulation type (CT) over the
463 BTH region. $PM_{2.5}$ concentrations in bold represent the mean/median value of each CT lower than the all-case
464 seasonal mean/median value.

| Seasonal Mean/ Median ($\mu g/m^3$) | CT1 | CT2 | CT3 | CT4 | CT5 | CT6 |
|---|---|---|---|---|---|---|
| 2013 (123.97/97.23) | **104.99/71.42** | **94.51/69.33** | 144.76/118.50 | 135.47/117.20 | 166.28/156.52 | **67.90/47.21** |
| 2014 (93.07/75.79) | **71.03/51.52** | 122.99/109.37 | 105.91/96.82 | **86.26/72.06** | 115.37/94.69 | 118.16/110.17 |
| 2015 (95.67/65.97) | **58.56/38** | **89.38**/73.07 | 134.77/114.69 | 135.91/106.36 | 124.15/99.81 | 106.14/70.63 |
| 2016 (112.94/91.32) | **84.74/66.16** | **110.02/88.10** | 138.96/114.26 | 122.86/95.02 | 142.52/128.77 | 132.95/129.52 |
| 2017 (70.44/54.07) | **56.49/43.16** | **60.70/39.61** | 80.03/67.39 | 83.89/67.24 | 93.63/79.28 | **69.77/52.23** |
| 2018 (79.85/63.02) | **77.99/60.68** | **51.77/37.43** | 89.26/77.57 | 86.70/81.35 | **75.08/52.72** | 108.60/93.02 |
| AVERAGE (95.27/72.22) | **73.14/53.04** | **79.12/54.89** | 115.18/96.29 | 109.85/88.25 | 116.04/89.04 | 100.40/82.04 |

465

466 Table 2. Regional mean meteorological variables over the BTH region under each circulation type

| Variables | CT1 | CT2 | CT3 | CT4 | CT5 | CT6 |
|---|---|---|---|---|---|---|
| Surface wind speed (m/s) | 3.27 | 2.31 | 2.71 | 2.24 | 2.58 | 2.54 |
| Surface wind speed anomaly (m/s) | 0.53 | -0.42 | -0.04 | -0.49 | -0.15 | -0.19 |
| Mean vertical velocity anomaly between 850 to 1000 hPa (pa/s) | 0.04 | -0.0358 | -0.0038 | -0.0296 | -0.0111 | -0.0213 |
| Difference of temperature anomaly between 850 and 1000 hPa (K) | -0.716 | -0.206 | 0.664 | 0.456 | 0.232 | 0.485 |

467

https://doi.org/10.5194/acp-2020-198
Preprint. Discussion started: 12 March 2020


Atmospheric Chemistry and Physics Discussions

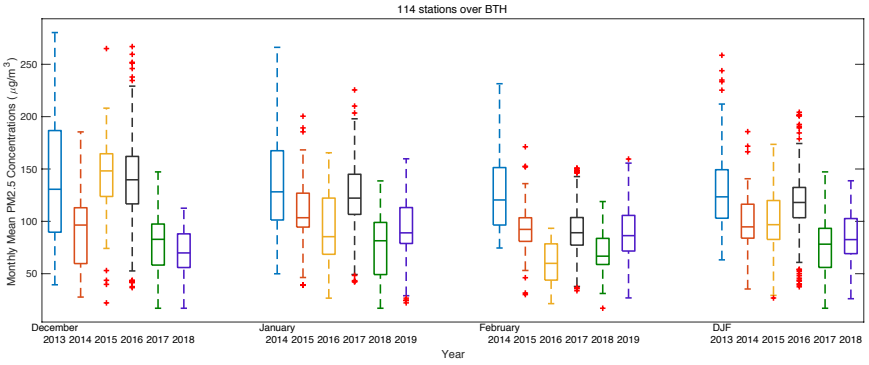


468

469 Figure 1. Interannual variation in the wintertime $PM_{2.5}$ concentrations at 114 stations over the BTH region. In each
470 box, the central mark indicates the median, and the bottom and top edges of the box indicate the 25th and 75th
471 percentiles, respectively. The whiskers extending to the most extreme data points are considered outliers. The region
472 covered by the blue box in Fig. 2 is considered as the BTH region (113º-117.5ºE and 36º-42ºN).

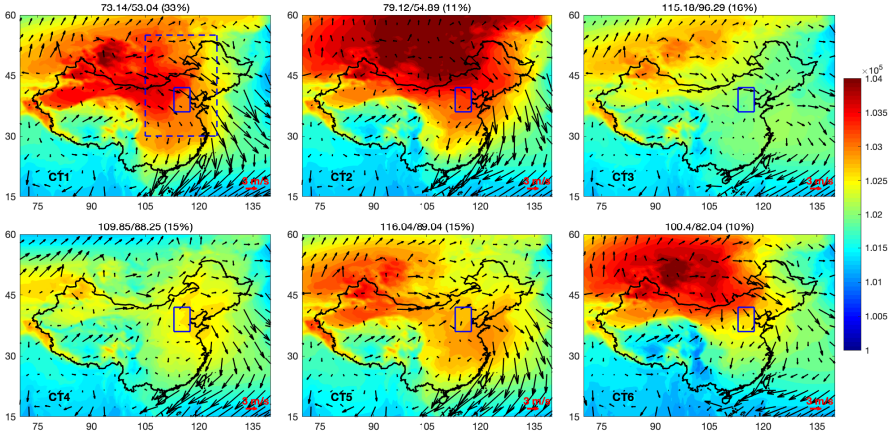


473

474 Figure 2. The distribution of sea level pressure (shaded, unit: pa) and 10 m wind fields (vector, unit: m/s) in each
475 circulation type. The number over each subplot indicates the occurrence frequency of the specific circulation type.
476 The solid blue box is the location of BTH region. The daily mean geopotential height fields at 925, 850 and 500 hPa
477 over the dashed blue box (105º-125ºE and 30º-55ºN) were applied to T-mode PCA method with the cost733 toolbox.
478 The region mean wind speed of each circulation type is shown in Table 2.

479

https://doi.org/10.5194/acp-2020-198
Preprint. Discussion started: 12 March 2020


Atmospheric Chemistry and Physics Discussions

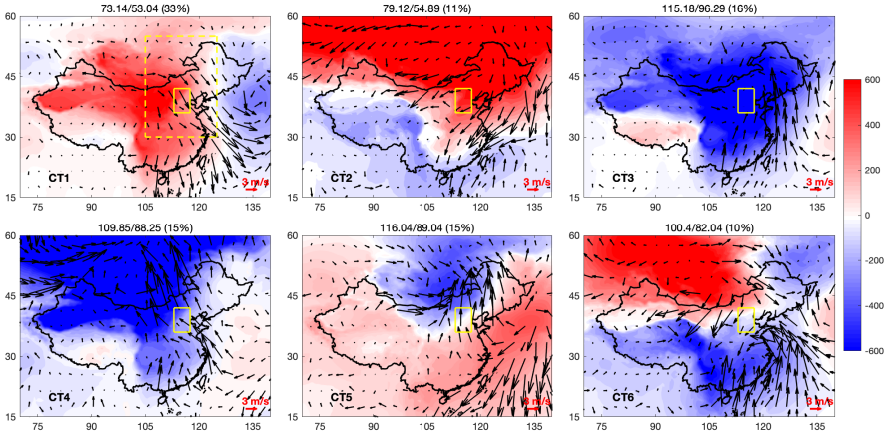


480

481 Figure 3. The distribution of sea level pressure (unit: pa) and 10 m wind fields (unit: m/s) anomaly in each circulation
482 type. The anomaly values are with respect to the 1980-2010 mean. Regional mean wind speed anomaly of each
483 circulation type is summarized in Table 2.

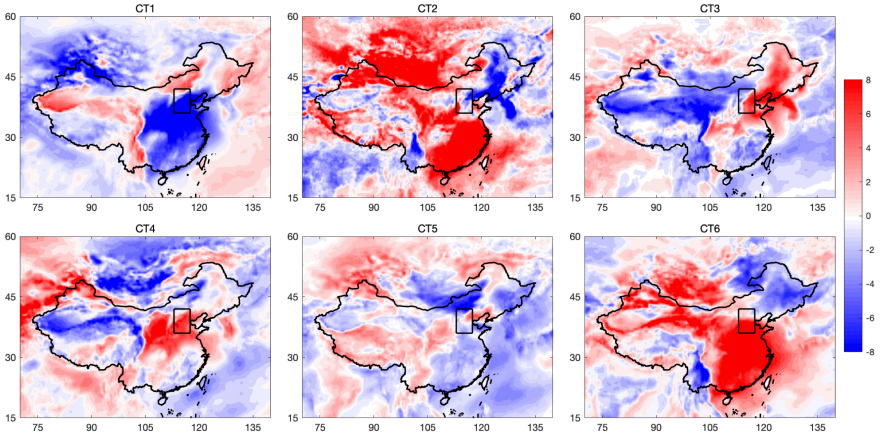


484

485 Figure 4. The distribution of relative humidity in each circulation type (unit: %). The anomaly values are with respect
486 to the 1980-2010 mean.

487

488

https://doi.org/10.5194/acp-2020-198
Preprint. Discussion started: 12 March 2020


Atmospheric Chemistry and Physics Discussions

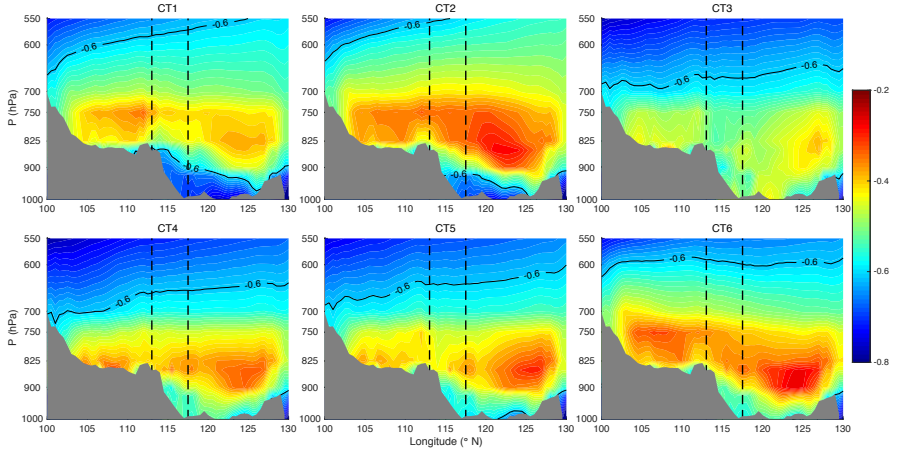


489

490 Figure 5. Zonal profile of temperature lapse rate over the BTH region (36º-42ºN) (unit: K/100 m). The gray region
491 indicates the average altitude over 36º-42ºN. The region between the two dashed lines is the horizontal location of
492 the BTH region (113º-117.5ºE).

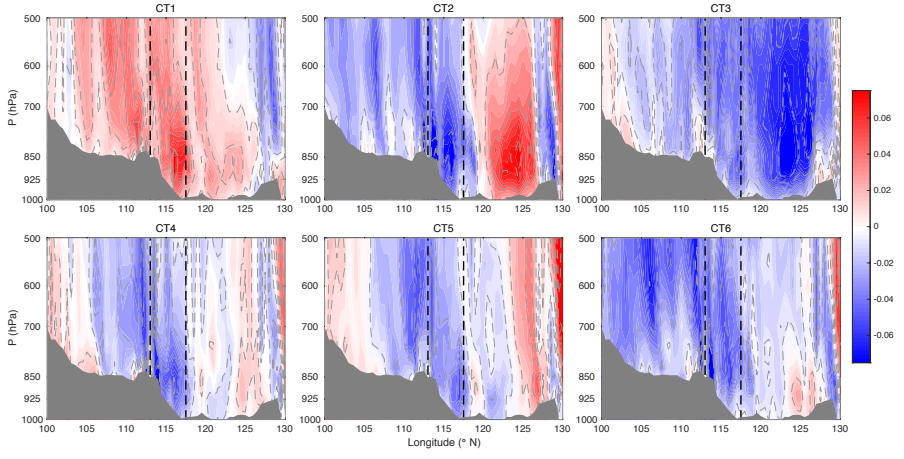


493

494 Figure 6. Zonal vertical profile of vertical velocity anomaly over BTH region (unit: pa/s). The anomaly of the vertical
495 velocities is with respect to the 1980 to 2010 mean value.

https://doi.org/10.5194/acp-2020-198
Preprint. Discussion started: 12 March 2020


Atmospheric Chemistry and Physics Discussions

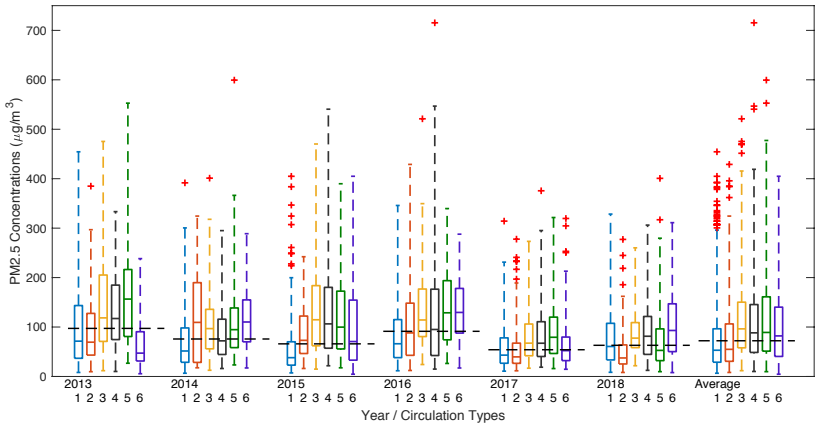


Figure 7. The box plot of the $PM_{2.5}$ concentrations varies with the circulation types. To exclude the effect of emission reduction on the annual mean $PM_{2.5}$ concentrations, the $PM_{2.5}$ distributions at the year and multiyear (average) scales are shown here, respectively. The dashed line for each year indicates the median $PM_{2.5}$ concentrations in wintertime of a specific year.

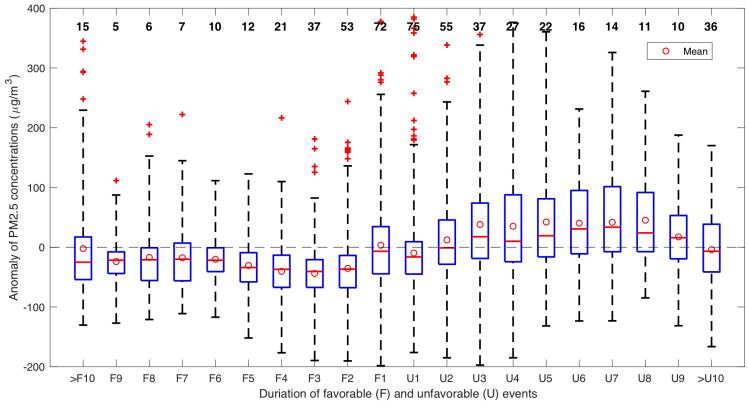


Figure 8. The daily $PM_{2.5}$ concentration anomalies vary with favorable (F) and unfavorable (U) event durations. The occurrences of CT1 and CT2 are collectively called favorable events, and CT3 to CT6 are referred to as unfavorable events. U1 indicates an unfavorable circulation event lasting for one day, and U2 means a two-day event. The central red line in each box indicates the median, and the circle is the mean value.

https://doi.org/10.5194/acp-2020-198
Preprint. Discussion started: 12 March 2020


Atmospheric Chemistry and Physics Discussions

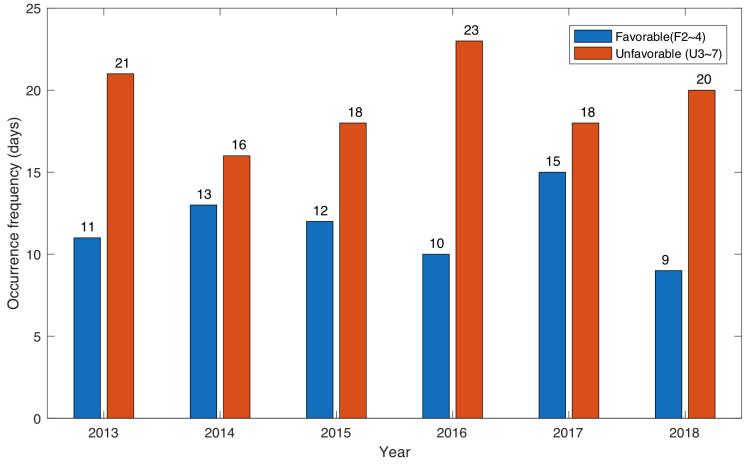


506

507 Figure 9. Occurrence frequencies of the effective favorable and unfavorable events. The effective favorable events
508 referred to the favorable events lasting for two to four days. The effective unfavorable events indicate the unfavorable
509 events lasting for three to seven days. The specific number of days for favorable/unfavorable events is shown on the
510 top of each bar.

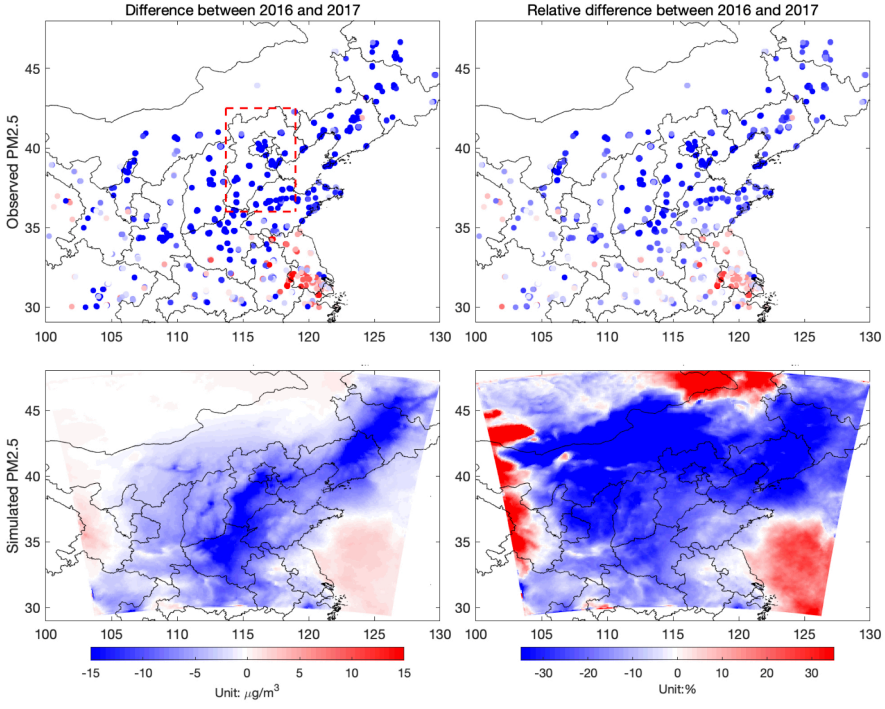


511

512 Figure 10. Distributions of the observed and simulated $PM_{2.5}$ difference between the winters of 2016 and 2017. The

https://doi.org/10.5194/acp-2020-198
Preprint. Discussion started: 12 March 2020


Atmospheric Chemistry and Physics Discussions

left panel is the absolute value (unit: μg/m$^3$) and the right panel is the relative difference with respect to the mean value of 2016 (unit: %). The simulated seasonal mean $PM_{2.5}$ concentrations during the two years are shown in Fig. S8.

https://doi.org/10.5194/acp-2020-198
Preprint. Discussion started: 12 March 2020


Atmospheric Chemistry and Physics Discussions

## Reference:

Ackermann, I. J., Hass, H., Memmesheimer, M., Ebel, A., Binkowski, F. S., and Shankar, U.: Modal aerosol dynamics model for Europe: Development and first applications, Atmospheric environment, 32, 2981-2999, 1998.

Bi, J., Huang, J., Holben, B. N., and Zhang, G.: Comparison of Key Absorption and Optical Properties Between Pure and Transported Anthropogenic Dust over East and Central Asia, Atmospheric Chemistry and Physics, 16, 15501-15516, 2016.

Cai, W., Li, K., Liao, H., and Wu, L.: Weather conditions conducive to Beijing severe haze more frequent under climate change, Nature Climate Change, 7, 257-262, 2017.

Cavazos, T.: Using self-organizing maps to investigate extreme climate events: An application to wintertime precipitation in the Balkans, Journal of climate, 13, 1718-1732, 2000.

Che, H., Xia, X., Zhao, H., Dubovik, O., Holben, B. N., Goloub, P., Cuevas-Agulló, E., Estelles, V., Wang, Y., and Zhu, J.: Spatial distribution of aerosol microphysical and optical properties and direct radiative effect from the China Aerosol Remote Sensing Network, Atmospheric Chemistry and Physics, 19, 11843-11864, 2019.

Chen, H., Wang, H., Sun, J., Xu, Y., and Yin, Z.: Anthropogenic fine particulate matter pollution will be exacerbated in eastern China due to 21st century GHG warming, Atmospheric Chemistry and Physics, 19, 233-243, 2019a.

Chen, S., Zhang, X., Lin, J., Huang, J., Zhao, D., Yuan, T., Huang, K., Luo, Y., Jia, Z., and Zang, Z.: Fugitive Road Dust $PM_{2.5}$ Emissions and Their Potential Health Impacts, Environmental Science & Technology, 53, 8455-8465, 2019b.

Chen, Z., Chen, D., Kwan, M.-P., Chen, B., Gao, B., Zhuang, Y., Li, R., and Xu, B.: The control of anthropogenic emissions contributed to 80% of the decrease in PM 2.5 concentrations in Beijing from 2013 to 2017, Atmospheric Chemistry and Physics, 19, 13519-13533, 2019c.

Notice of the General Office of the State Council on Issuing the Air Pollution Prevention and Control Action Plan: http://www.gov.cn/zwgk/2013-09/12/ content_2486773.htm, access: 30/12/2019, 2013.

The State Council rolls out a three-year action plan for clean air: http://www.gov.cn/zhengce/content/2018-07/03/content_5303158.htm, access: 30/12/2019, 2018.

Collins, W. D., Rasch, P. J., Boville, B. A., Hack, J. J., McCaa, J. R., Williamson, D. L., Kiehl, J. T., Briegleb, B., Bitz, C., and Lin, S.-J.: Description of the NCAR community atmosphere model (CAM 3.0), NCAR Tech. Note NCAR/TN-464+ STR, 226, 2004.

Dang, R., and Liao, H.: Severe winter haze days in the Beijing–Tianjin–Hebei region from 1985 to 2017 and the roles of anthropogenic emissions and meteorology, Atmospheric Chemistry and Physics, 19, 10801-10816, 2019.

Ding, A., Huang, X., Nie, W., Chi, X., Xu, Z., Zheng, L., Xu, Z., Xie, Y., Qi, X., Shen, Y., Sun, P., Wang, J., Wang, L., Sun, J., Yang, X. Q., Qin, W., Zhang, X., Cheng, W., Liu, W., Pan, L., and Fu, C.: Significant reduction of $PM_{2.5}$ in eastern China due to regional-scale emission control: evidence from SORPES in 2011–2018, Atmos. Chem. Phys., 19, 11791-11801, 10.5194/acp-19-11791-2019, 2019.

https://doi.org/10.5194/acp-2020-198
Preprint. Discussion started: 12 March 2020


Atmospheric Chemistry and Physics Discussions

552 Fan, H., Zhao, C., and Yang, Y.: A comprehensive analysis of the spatio-temporal variation of urban air pollution in
553 China during 2014–2018, Atmospheric Environment, 220, 117066, 2020.

554 Feng, J., Li, J., Liao, H., and Zhu, J.: Simulated coordinated impacts of the previous autumn North Atlantic
555 Oscillation (NAO) and winter El Niño on winter aerosol concentrations over eastern China, Atmospheric Chemistry
556 and Physics, 19, 10787-10800, 2019.

557 Gui, K., Che, H., Wang, Y., Wang, H., Zhang, L., Zhao, H., Zheng, Y., Sun, T., and Zhang, X.: Satellite-derived PM2.
558 5 concentration trends over Eastern China from 1998 to 2016: Relationships to emissions and meteorological
559 parameters, Environmental pollution, 247, 1125-1133, 2019.

560 Guo, J., Xu, H., Liu, L., Chen, D., Peng, Y., Yim, S. H. L., Yang, Y., Li, J., Zhao, C., and Zhai, P.: The trend reversal
561 of dust aerosol over East Asia and the North Pacific Ocean attributed to large-scale meteorology, deposition and soil
562 moisture, Journal of Geophysical Research: Atmospheres, 2019.

563 He, J., Lu, S., Yu, Y., Gong, S., Zhao, S., and Zhou, C.: Numerical Simulation Study of Winter Pollutant Transport
564 Characteristics over Lanzhou City, Northwest China, Atmosphere, 9, 382, 2018.

565 Hong, C., Zhang, Q., Zhang, Y., Davis, S. J., Tong, D., Zheng, Y., Liu, Z., Guan, D., He, K., and Schellnhuber, H. J.:
566 Impacts of climate change on future air quality and human health in China, Proceedings of the National Academy
567 of Sciences, 116, 17193-17200, 2019.

568 Huang, X., Wang, Z., and Ding, A.: Impact of Aerosol-PBL Interaction on Haze Pollution: Multiyear Observational
569 Evidences in North China, Geophysical Research Letters, 45, 8596-8603, 2018.

570 Huth, R.: A circulation classification scheme applicable in GCM studies, Theoretical and applied climatology, 67,
571 1-18, 2000.

572 Huth, R., Beck, C., Philipp, A., Demuzere, M., Ustrnul, Z., Cahynová, M., Kyselý, J., and Tveito, O. E.:
573 Classifications of atmospheric circulation patterns: recent advances and applications, Annals of the New York
574 Academy of Sciences, 1146, 105-152, 2008.

575 Iacono, M. J., Delamere, J. S., Mlawer, E. J., Shephard, M. W., Clough, S. A., and Collins, W. D.: Radiative forcing
576 by long-lived greenhouse gases: Calculations with the AER radiative transfer models, Journal of Geophysical
577 Research: Atmospheres, 113, 2008.

578 Janjić, Z. I.: The Step-Mountain Eta Coordinate Model: Further Developments of the Convection, Viscous Sublayer,
579 and Turbulence Closure Schemes, Monthly Weather Review, 122, 927-945, 10.1175/1520-
580 0493(1994)122<0927:TSMECM>2.0.CO;2, 1994.

581 Leung, D. M., Tai, A. P., Mickley, L. J., Moch, J. M., Donkelaar, A. v., Shen, L., and Martin, R. V.: Synoptic
582 meteorological modes of variability for fine particulate matter (PM 2.5) air quality in major metropolitan regions of
583 China, Atmospheric Chemistry and Physics, 18, 6733-6748, 2018.

584 Li, G., Zavala, M., Lei, W., Tsimpidi, A., Karydis, V., Pandis, S. N., Canagaratna, M., and Molina, L.: Simulations
585 of organic aerosol concentrations in Mexico City using the WRF-CHEM model during the MCMA-2006/MILAGRO
586 campaign, Atmospheric Chemistry and Physics, 11, 3789-3809, 2011.

587 Li, J., Lv, Q., Jian, B., Zhang, M., Zhao, C., Fu, Q., Kawamoto, K., and Zhang, H.: The impact of atmospheric
588 stability and wind shear on vertical cloud overlap over the Tibetan Plateau, Atmospheric Chemistry and Physics, 18,

https://doi.org/10.5194/acp-2020-198
Preprint. Discussion started: 12 March 2020




589 7329-7343, 2018.

590 Li, J., Liao, H., Hu, J., and Li, N.: Severe particulate pollution days in China during 2013–2018 and the associated
591 typical weather patterns in Beijing-Tianjin-Hebei and the Yangtze River Delta regions, Environmental pollution, 248,
592 74-81, 2019.

593 Li, Q., Zhang, R., and Wang, Y.: Interannual variation of the wintertime fog–haze days across central and eastern
594 China and its relation with East Asian winter monsoon, International Journal of Climatology, 36, 346-354, 2016.

595 Liu, C., Chen, R., Sera, F., Vicedo-Cabrera, A. M., Guo, Y., Tong, S., Coelho, M. S., Saldiva, P. H., Lavigne, E., and
596 Matus, P.: Ambient particulate air pollution and daily mortality in 652 cities, New England Journal of Medicine, 381,
597 705-715, 2019.

598 Miao, Y., Guo, J., Liu, S., Liu, H., Li, Z., Zhang, W., and Zhai, P.: Classification of summertime synoptic patterns in
599 Beijing and their associations with boundary layer structure affecting aerosol pollution, Atmospheric Chemistry and
600 Physics, 17, 3097-3110, 2017.

601 Mu, M., and Zhang, R.: Addressing the issue of fog and haze: A promising perspective from meteorological science
602 and technology. Science China Earth Science, 57, 1–2, 2017.

603 Philipp, A., Beck, C., Esteban, P., Kreienkamp, F., Krennert, T., Lochbihler, K., Lykoudis, S. P., Pianko-Kluczynska,
604 K., Post, P., and Alvarez10, D. R.: cost733class-1.2 User guide, Augsburg, Germany, 10-21, 2014.

605 Schell, B., Ackermann, I. J., Hass, H., Binkowski, F. S., and Ebel, A.: Modeling the formation of secondary organic
606 aerosol within a comprehensive air quality model system, Journal of Geophysical Research: Atmospheres, 106,
607 28275-28293, 2001.

608 Song, Z., Fu, D., Zhang, X., Wu, Y., Xia, X., He, J., Han, X., Zhang, R., and Che, H.: Diurnal and seasonal variability
609 of PM2. 5 and AOD in North China plain: Comparison of MERRA-2 products and ground measurements,
610 Atmospheric environment, 191, 70-78, 2018.

611 Stockwell, W. R., Middleton, P., Chang, J. S., and Tang, X.: The second generation regional acid deposition model
612 chemical mechanism for regional air quality modeling, Journal of Geophysical Research: Atmospheres, 95, 16343-
613 16367, 1990.

614 Tao, S., Ru, M. Y., Du, W., Zhu, X., Zhong, Q. R., Li, B. G., Shen, G. F., Pan, X. L., Meng, W. J., Chen, Y. L., Shen,
615 H. Z., Lin, N., Su, S., Zhuo, S. J., Huang, T. B., Xu, Y., Yun, X., Liu, J. F., Wang, X. L., Liu, W. X., Cheng, H. F.,
616 and Zhu, D. Q.: Quantifying the rural residential energy transition in China from 1992 to 2012 through a
617 representative national survey, Nature Energy, 3, 567-573, 10.1038/s41560-018-0158-4, 2018.

618 Tie, X., Zhang, Q., He, H., Cao, J., Han, S., Gao, Y., Li, X., and Jia, X. C.: A budget analysis of the formation of
619 haze in Beijing, Atmospheric Environment, 100, 25-36, 2015.

620 Valverde, V., Pay, M. T., and Baldasano, J. M.: Circulation-type classification derived on a climatic basis to study
621 air quality dynamics over the Iberian Peninsula, International Journal of Climatology, 35, 2877-2897, 2015.

622 Wang, K., Dickinson, R. E., and Liang, S.: Clear sky visibility has decreased over land globally from 1973 to 2007,
623 Science, 323, 1468-1470, 2009.

624 Wang, X., Wang, K., and Su, L.: Contribution of atmospheric diffusion conditions to the recent improvement in air

https://doi.org/10.5194/acp-2020-198
Preprint. Discussion started: 12 March 2020


Atmospheric Chemistry and Physics Discussions

quality in China, Scientific reports, 6, 36404, 2016.

Wang, X., Wen, H., Shi, J., Bi, J., Huang, Z., Zhang, B., Zhou, T., Fu, K., Chen, Q., and Xin, J.: Optical and microphysical properties of natural mineral dust and anthropogenic soil dust near dust source regions over northwestern China, Atmospheric Chemistry and Physics, 18, 2119-2138, 2017.

Wang, X., Dickinson, R. E., Su, L., Zhou, C., and Wang, K.: PM2. 5 pollution in China and how it has been exacerbated by terrain and meteorological conditions, Bulletin of the American Meteorological Society, 99, 105-119, 2018.

Wang, X., Zhang, R., and Yu, W.: The effects of $PM_{2.5}$ concentrations and relative humidity on atmospheric visibility in Beijing, Journal of Geophysical Research: Atmospheres, 124, 2235-2259, 2019a.

Wang, Y., Li, W., Gao, W., Liu, Z., Tian, S., Shen, R., Ji, D., Wang, S., Wang, L., and Tang, G.: Trends in particulate matter and its chemical compositions in China from 2013–2017, Science China Earth Sciences, 1-15, 2019b.

Xu, J., Chang, L., Qu, Y., Yan, F., Wang, F., and Fu, Q.: The meteorological modulation on PM2. 5 interannual oscillation during 2013 to 2015 in Shanghai, China, Science of The Total Environment, 572, 1138-1149, 2016.

Yin, Z., Wang, H., and Ma, X.: Possible Relationship between the Chukchi Sea Ice in the Early Winter and the February Haze Pollution in the North China Plain, Journal of Climate, 32, 5179-5190, 2019.

Zhai, S., Jacob, D. J., Wang, X., Shen, L., Li, K., Zhang, Y., Gui, K., Zhao, T., and Liao, H.: Fine particulate matter ($PM_{2.5}$) trends in China, 2013–2018: separating contributions from anthropogenic emissions and meteorology, Atmos. Chem. Phys., 19, 11031-11041, 10.5194/acp-19-11031-2019, 2019.

Zhang, J. P., Zhu, T., Zhang, Q., Li, C., Shu, H., Ying, Y., Dai, Z., Wang, X., Liu, X., and Liang, A.: The impact of circulation patterns on regional transport pathways and air quality over Beijing and its surroundings, Atmospheric Chemistry and Physics, 12, 5031-5053, 2012.

Zhang, Q., Jiang, X., Tong, D., Davis, S. J., Zhao, H., Geng, G., Feng, T., Zheng, B., Lu, Z., and Streets, D. G.: Transboundary health impacts of transported global air pollution and international trade, Nature, 543, 705, 2017.

Zhang, Q., and Geng, G.: Impact of clean air action on PM 2.5 pollution in China, in, Springer, 2019.

Zhang, Q., Zheng, Y., Tong, D., Shao, M., Wang, S., Zhang, Y., Xu, X., Wang, J., He, H., and Liu, W.: Drivers of improved PM2. 5 air quality in China from 2013 to 2017, Proceedings of the National Academy of Sciences, 116, 24463-24469, 2019a.

Zhang, R., Li, Q., and Zhang, R.: Meteorological conditions for the persistent severe fog and haze event over eastern China in January 2013, Science China Earth Sciences, 57, 26-35, 2014.

Zhang, R.: Atmospheric science: Warming boosts air pollution, Nature Climate Change, 7, 238-239, 2017.

Zhang, X., Xu, X., Ding, Y., Liu, Y., Zhang, H., Wang, Y., and Zhong, J.: The impact of meteorological changes from 2013 to 2017 on PM 2.5 mass reduction in key regions in China, Science China Earth Sciences, 1-18, 2019b.

Zhang, Y., Vu, V. T., Sun, J., He, J., Shen, X., Lin, W., Zhang, X., Zhong, J., Gao, W., and Wang, Y.: Significant changes in chemistry of fine particles in wintertime Beijing from 2007 to 2017: Impact of clean air actions, Environmental science & technology, 2019c.

https://doi.org/10.5194/acp-2020-198
Preprint. Discussion started: 12 March 2020


Atmospheric Chemistry and Physics Discussions

660 Zhao, B., Zheng, H., Wang, S., Smith, K. R., Lu, X., Aunan, K., Gu, Y., Wang, Y., Ding, D., and Xing, J.: Change in
661 household fuels dominates the decrease in PM2. 5 exposure and premature mortality in China in 2005–2015,
662 Proceedings of the National Academy of Sciences, 115, 12401-12406, 2018a.

663 Zhao, C., Wang, Y., Shi, X., Zhang, D., Wang, C., Jiang, J. H., Zhang, Q., and Fan, H.: Estimating the Contribution
664 of Local Primary Emissions to Particulate Pollution Using High-Density Station Observations, Journal of
665 Geophysical Research: Atmospheres, 124, 1648-1661, 2019a.

666 Zhao, C., Yu, Y., Kuang, Y., Tao, J., and Zhao, G.: Recent progress of aerosol light-scattering enhancement factor
667 studies in China, Advances in Atmospheric Sciences, 36, 1015-1026, 2019b.

668 Zhao, H., Che, H., Xia, X., Wang, Y., Wang, H., Wang, P., Ma, Y., Yang, H., Liu, Y., and Wang, Y.: Multiyear Ground-
669 Based Measurements of Aerosol Optical Properties and Direct Radiative Effect Over Different Surface Types in
670 Northeastern China, Journal of Geophysical Research: Atmospheres, 123, 13,887-813,916, 2018b.

671 Zhao, S., Zhang, H., and Xie, B.: The effects of El Niño–Southern Oscillation on the winter haze pollution of China,
672 Atmospheric Chemistry and Physics, 18, 1863, 2018c.

673 Zheng, B., Tong, D., Li, M., Liu, F., Hong, C., Geng, G., Li, H., Li, X., Peng, L., and Qi, J.: Trends in China's
674 anthropogenic emissions since 2010 as the consequence of clean air actions, Atmospheric Chemistry and Physics,
675 18, 14095-14111, 2018.

676 Zhong, Q., Ma, J., Shen, G., Shen, H., Zhu, X., Yun, X., Meng, W., Cheng, H., Liu, J., Li, B., Wang, X., Zeng, E. Y.,
677 Guan, D., and Tao, S.: Distinguishing Emission-Associated Ambient Air $PM_{2.5}$ Concentrations and Meteorological
678 Factor-Induced Fluctuations, Environmental Science & Technology, 52, 10416-10425, 10.1021/acs.est.8b02685,
679 2018.

680

681

682